Chapter 5

Commented [PN1]:

Thermal-fluids

5.1 Preliminary studies

This section carries out some preliminary studies using Moltres and MOOSE heat conduction modules to solve the prismatic HTGR thermal-fluids.

Commented [PN2]: various –change for style

Commented [PN3]: make plural

Commented [PN4]: spell out first instance

5.1.1 Verification of the thermal-fluids model

To verify our methodology, this section solved a simplified cylindrical model whose analytical solution we know~~.~~ (see Section 8.1 for a presentation on this solution). ~~presents the problem's analytical solution.~~ Moltres/MOOSE obtained the numerical solution of the thermal-fluid equations from Section 3.2.2.

Commented [PN5]: are these the same thing? If so, state that. Otherwise, specify what the / means. Were they used together?

Figure 5.1 displays the model geometry, which differentiates five subregions: fuel compact, helium gap, moderator, film, and coolant. Table 5.1 summarizes the geometry dimensions and the input parameters. The model reference design was the GT-MHR. The calculated moderator radius is the fuel/coolant pitch minus the fuel compact and coolant channel radii — the minimum distance between the fuel and coolant channels in the unit cell. We obtained the calculated coolant radius by preserving the coolant channel volume. The model assumed a sinusoidal power profile in the *z*-direction.

Commented [PN6]: spell out first instance

Commented [PN7]: can this be inserted as an equation? might be clearer for reader. if so, cut and "This value is given by: (equation here), where (explain variables here)."

Figure 5.2 shows the axial and radial temperature profiles and demonstrates that b~~. B~~oth the analytical and numerical solutions exhibit good agreement. The outlet coolant temperature is 770.2 ◦C, whereas the average outlet coolant temperature of the reference reactor is 950 ◦C. Note that this is a simplified model only for verifying that the numerical solution agrees with the analytical solution. The model also considers only one fuel channel, while in the GT-MHR unit cell, two fuel channels deposit their heat into one coolant channel.

Commented [PN8]: can you clarify here why this doesn't drastically affect your analysis? seems like something that would be a big deal, but I also have no idea why.

5.1.2 Unit cell problem

This section solved the unit cell problem in the hot spot of an HTGR. We intended to reproduce the results found by In et al. 2006 [53] to validate the unit-cell model. We chose this article because it solves a three-dimensional unit-cell model and gives one of the most thorough descriptions in the open literature. Table 5.2 presents the problem characteristics.

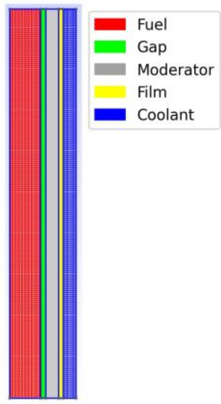

Figure 5.1: Scaled-down version of the model geometry.

Table 5.1: Problem characteristics.

Parameter	Symbol	Value	Units	Reference
Fuel compact radius	R_f	0.6225	cm	[53]
Fuel channel radius	R_g	0.6350	cm	[53]
Coolant channel radius	-	0.7950	cm	[53]
Fuel/coolant pitch	-	1.8850	cm	[53]
Fuel column height	L	793	cm	[53]
Coolant mass flow rate	$\dot{m}$	0.0176	kg/s	[53]
Average power density	q_{ave}	35	W/cm^3	[53]
Coolant inlet temperature	T_{in}	400	$^\circ C$	[53]
Helium inlet pressure	P	70	bar	[53]
Helium density	ρ_c	4.940×10^{-6}	kg/cm^3	[91]
Helium heat capacity	$c_{p,c}$	5188	J/kg/K	[91]
Fuel compact thermal conductivity	k_f	0.07	W/cm/K	[118]
Gap thermal conductivity	k_g	3×10^{-3}	W/cm/K	[118]
Moderator thermal conductivity	k_m	0.30	W/cm/K	[118]
Calculated parameters				
Calculated moderator radius	R_m	1.080	cm	-
Coolant film radius	R_i	1.090	cm	-
Calculated coolant radius	R_c	1.349	cm	-
Coolant average velocity	v_c	1794.33	cm/s	-
Film thermal conductivity	k_i	1.722×10^{-3}	W/cm/K	-

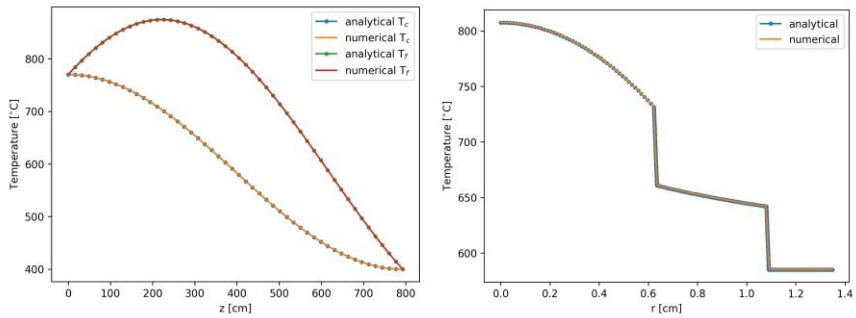

(a) Fuel centerline and bulk coolant axial temperatures.   (b) Radial temperature at z=L/2=396.5 cm.

Figure 5.2: Temperature profiles.

The article does not specify the solid's material properties, ~~and~~ so we ~~replaced them with parameters~~used parameters from Tak et al. 2008 [118]. Figure 5.3 displays an *XY* -plane of the model geometry and the material properties that depend on the temperature. Additionally, In et al. used a chopped cosine as the power profile, which ~~. To simplify the analysis,~~ we used the average value of~~-~~ to simplify the analysis.~~the power profile~~.

Commented [PN9]: if there were no specifications to start with, what got replaced?

Table 5.2: Problem characteristics.

Parameter	Symbol	Value	Units	Reference
Fuel compact radius	R_f	0.6225	cm	[53]
Fuel channel radius	R_g	0.6350	cm	[53]
Coolant channel radius	R_c	0.7950	cm	[53]
Fuel/coolant pitch	p	1.8850	cm	[53]
Fuel column height	L	793	cm	[53]
Coolant channel mass flow rate	$\dot{m}$	0.0176	kg/s	[53]
Average power density	q_{ave}	35	W/cm³	[53]
Inlet coolant temperature	T_{in}	400	°C	[53]
Helium inlet pressure	P	70	bar	[53]
Helium density	ρ	4.94×10^{-6}	kg/cm³	[91]
Helium heat capacity	c_p	5188	J/kg/K	[91]
Calculated parameters				
Coolant film radius	R_i	0.8050	cm	-
Coolant average velocity	v_c	1794.33	cm/s	-
Film thermal conductivity	k_i	1.731×10^{-3}	W/cm/K	-

Figure 5.4 shows the temperature profiles. From the top to the bottom of the reactor, the axial temperatures increase, the moderator and coolant temperatures remain parallel (the model assumes a film thermal conductivity independent of temperature), and the differences between the fuel and moderator temperatures decrease ~~The axial temperatures increase from the top to the bottom of the reactor. The moderator and coolant temperatures are parallel as the model assumes a film thermal~~

Commented [PN10]:

~~conductivity independent of the temperature. The fuel and moderator temperature difference decreases.~~ As the different materials' thermal conductivity increases with temperature, the thermal resistance between the moderator and

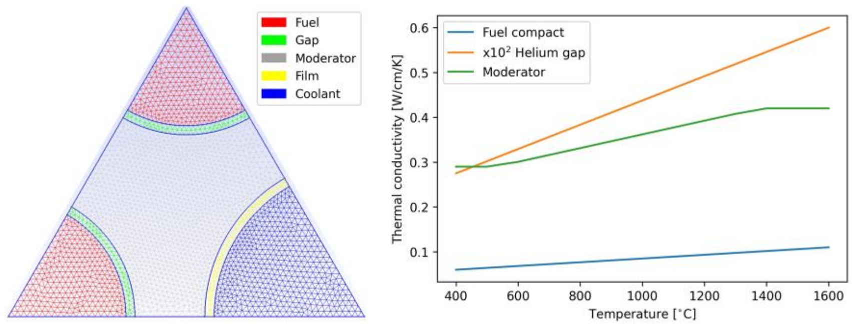

(a) Model geometry. (b) Material properties.

Figure 5.3: Moltres/MOOSE input parameters.

the fuel decreases. Table 5.3 summarizes the results.

There are several temperature discrepancies in our calculations: Moltres/MOOSE coolant temperature is smaller by 4°C, t~~. T~~he moderator temperature is larger by 9°C, and t~~. T~~he fuel temperature is larger by 22°C. The cause of the fuel temperature discrepancies~~y~~ is the power profile simplification. As we have seen in the previous section, the fuel-to-coolant temperature difference is small in the outlet for a sinusoidal power profile. The opposite extreme scenario is the uniform power profile, where the fuel-to-coolant temperature difference is larger. In et al. used a chopped cosine power profile, which is ~~the case in~~ between the two former cases~~a uniform and a sinusoidal power profile~~. Hence, our model yields a larger fuel-to-coolant temperature at the outlet. Overall, our ~~model~~ results agreed ~~showed good agreement~~ with In et al.

results.

Commented [PN11]: smaller than In et al.? might need to specify here

Formatted: Indent: First line: 0.5"

Commented [PN12]: larger than In et al.? specify here too

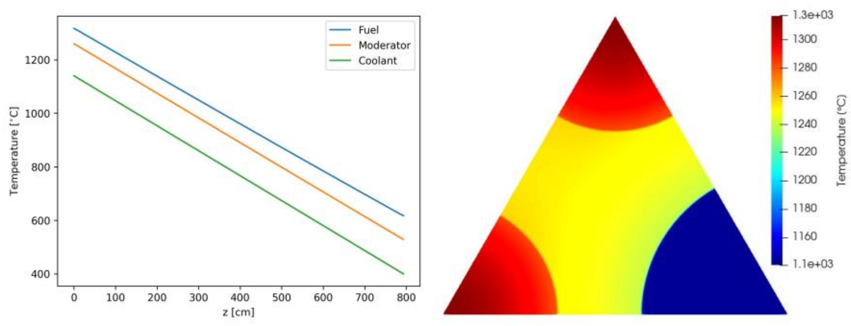

(a) Maximum fuel, moderator, and bulk coolant axial tempera- (b) Outlet plane temperature z=793 cm. tures.

Figure 5.4: Temperature profiles.

Table 5.3: Comparison between In et al. and Moltres/MOOSE results.

Parameter	In et al.	Moltres/MOOSE
Maximum coolant temperature [°C]	1144	1140
Maximum moderator temperature [°C]	1250	1259
Maximum fuel temperature [°C]	1295	1317

5.2 Fuel column

This section solved an HTGR fuel column and~~. It~~ aimed to reproduce some of Sato et al. 2010 [107] analyses to validate the fuel column model. We chose this article because it gives a thorough description of the problem, making it easier to reproduce. First, we analyzed a column with no bypass-gap. Second, we studied a column with a 3mm-gap. The study used the GT-MHR as the reference reactor for the calculations;~~.~~ Figure 5.5a ~~a~~exhibits the model geometry. The model ~~included~~ only needed to include a one-twelfth portion of the column due to symmetry. The GT-MHR shares the geometry dimensions with the MHTGR, which Table 3.2 specifies.

Commented [PN13]: this could very well just be me not knowing what this means, but what do you mean by "solve" a fuel column?

For background: Equation 5.1 evaluates the solid material properties [60],~~.~~ Table 5.5 displays the fuel compact and moderator thermal conductivity coefficients,~~.~~ Table 5.4 lists the helium properties and several input parameters, and~~.~~ Figure 5.5b shows the temperature-dependent material properties.

Commented [PN14]: This seemed a little choppy but could definitely be left as is. Just a style thing.

$$\varphi(T) = A_1 + A_2 T + A_3 T^{2} + A_4 T^{3} + A_5 T^{4} \tag{5.1}$$

The model assigns a number to each coolant channel and the bypass-gap~~,~~ (see Figure 5.5a). In this exercise, we use the mass flow distribution from Sato et al. Table 5.6 shows the mass flow rate in each channel.

Table 5.4: Problem characteristics.

Parameter	Symbol	Value	Units	Reference
Inlet coolant temperature	T_{in}	490	°C	[107]
Helium inlet pressure	P	70	bar	[107]
Helium density	ρ	4.37×10^{-6}	kg/cm^3	[91]
Helium heat capacity	c_p	5188	J/kg/K	[91]
Average power density	q_{ave}	27.88	W/cm^3	[107]
Calculated parameters				
Coolant film radius	R_i	0.804	cm	-
Film thermal conductivity	k_i	2.09×10^{-3}	W/cm/K	-

Table 5.7 compares Moltres/MOOSE results to Sato's results. In the no gap case, Moltres/MOOSE's maximum coolant temperature is 2 °C lower, and the maximum fuel temperature is 4 °C higher. In the 3mm-gap case, Table 5.5: Thermal conductivity coefficients.

Commented [PN15]: I'm assuming this is just a Word formatting glitch, but maybe double check on the original doc just in case

	Moderator			Fuel compact
Temperature range [K]	255.6-816	816-1644.4	1644.4-1922.2	255.6-2200
A1	28.6	1.24E+2	41.5	3.94
A2	-	-3.32E-1	-	3.59E-3
A3	-	4.09E-4	-	-1.98E-9
A4	-	-2.11E-7	-	3.19E-12
A5	-	4.02E-11	-	-9.77E-16

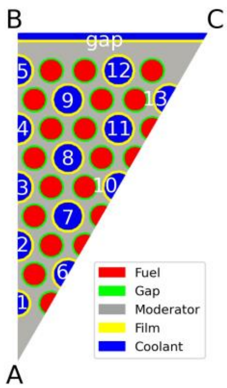

(a) Model geometry.

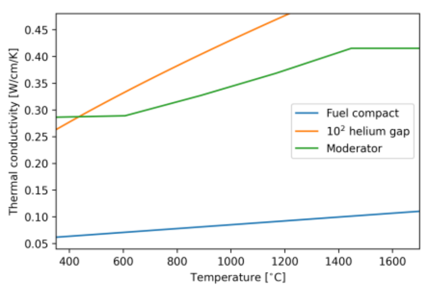

(b) Material properties.

Table 5.6: Mass flow rate [g/s]. Values form [107].

Channel	1	2	3	4	5	6	7
No gap	6.18	11.34	11.37	11.38	11.43	11.33	22.70
3mm gap	5.88	10.80	10.85	10.91	11.08	10.80	21.58
Channel	**8**	**9**	**10**	**11**	**12**	**13**	**Gap**
No gap	22.73	22.73	11.38	22.77	22.91	11.44	-
3mm gap	21.67	21.83	10.88	21.81	22.20	11.10	16.56

Moltres/MOOSE's maximum coolant temperature is 2 ◦C lower, and the maximum fuel temperature is 1◦C lower. The results showed good agreement.

Commented [PN16]: with Sato? specify

Figure 5.5 displays the outlet temperature along lines A-B and A-C from Figure 5.5a. The temperature is higher closer to the column center, because the~~. The~~ bypass-flow causes the temperature in the center to rise while reducing the peripheral temperature. The presence of the gap produces a larger temperature gradient in the assembly.

Commented [PN17]: temperature gap or physical gap?

Table 5.7: Maximum temperatures.

	No gap		3mm gap	
	Sato et al.	Moltres/MOOSE	Sato et al.	Moltres/MOOSE
Bulk coolant	985	983	1007	1005
Fuel	1090	1094	1115	1114

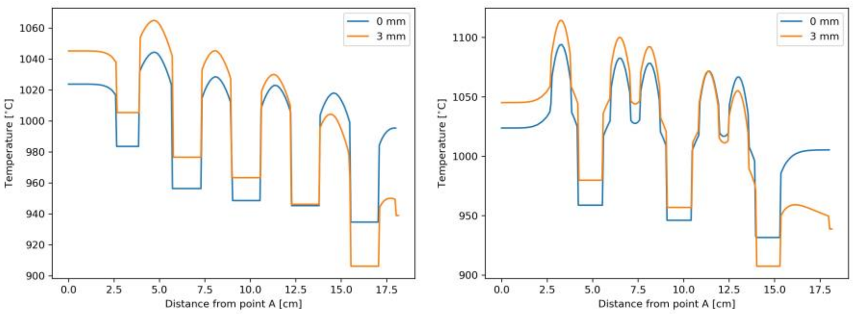

(a) Line A-B.

(b) Line A-C.

Figure 5.5: Outlet plane temperature along the line A-B and line A-C.

5.2.1 Flow distribution analysis

As described in Section 2.2, several authors calculate the flow distribution using various methods. This section compares the different method results. The comparison chosen metrics are the maximum coolant and fuel temperatures and the mass flow distribution The model assigns a number to each coolant channel and the bypass-gap~~,~~ (see Figure 5.5a). Note that C~~c~~hannel 1 is a small coolant channel while C~~c~~hannels 2 to 13 are large coolant channels.

We analyzed the following cases:

- Case 1: uses the mass flow distribution from Sato et al.
- Case 2: uses a flat velocity profile (every channel and gap have the same velocity).
- Case 3: uses the incompressible flow model with a temperature-independent helium viscosity.
- Case 4: uses the incompressible flow model with a temperature-dependent helium viscosity.

- Case 5: uses the low-Mach number model with a temperature dependent helium viscosity.

To calculate the different flow distributions, we used the following equations~~:~~. Equation 5.2 calculated the flow distribution in C~~c~~ase 1. Equation 5.3 [84] calculated the pressure drop in C~~c~~ases 3 and 4. Case 4 differs from C~~c~~ase 3 as the friction factor *f* depends on the average channel temperature. Equation 5.4 [84] calculated the pressure drop in C~~c~~ase 5. For C~~c~~ases 3 to 5, the pressure drop is proportional to the channel mass flow~~,~~ (E~~e~~quation 5.5). Equations 5.3 and 5.4 calculated B_i. Equations 5.6 and 5.7 [84] solved the mass flow distribution iteratively. As the mass flow distributions in C~~c~~ases 4 and 5 ~~mass flow distributions~~ depend on ~~the~~ temperature, the calculations required another level of iterations to obtain the final mass flow distribution. The convergence criteria were 1◦C for the maximum coolant and fuel temperatures.

Commented [PN18]: maybe consider reformatting part of this section as a list/using bullet points? it seems like that might be a clearer way to convey the information, but is also fine as is

$$\dot{m}_i = \frac{A_i}{\sum_j A_j} \tag{5.2}$$

$$\Delta P = \frac{1}{\rho}\left(\frac{\dot{m}_i}{A_i}\right)^2 f\,\frac{2L}{D_h} \tag{5.3}$$

$$\Delta P = \frac{\dot{m}_i^2}{2\rho A_i^2}\left(\frac{4fL(T_i+T_o)}{2DT_i}+\frac{T_o-T_i}{T_i}\right) \tag{5.4}$$

$$\Delta P = B_i \dot{m}_i^2 \tag{5.5}$$

$$\Delta P = \left(\frac{\dot{m}_T}{\sum_i \frac{1}{\sqrt{B_i}}}\right)^2 \tag{5.6}$$

$$\dot{m}_i = \sqrt{\Delta P / B_i} \tag{5.7}$$

where

$\dot{m}_i$ = channel *i* mass flow rate

A_i = channel *i* cross-sectional area

ΔP = pressure drop

T_i = channel inlet coolant temperature

T_o = channel outlet coolant temperature $\dot{m}_T$ =

total mass flow rate

(5.8)

Table 5.8 displays the results for the mass flow rates. Case 2 yields the largest small coolant channel mass flow and the smallest large coolant channel mass flow. Case 3 and 4 barely differ. Not considering the viscosity's temperature dependency yields a more straightforward method and the accuracy loss is negligible. Case 5 arrives at the closest values to the reference solution.

Table 5.9 summarizes the maximum temperatures. Case 2 yields the largest difference for the maximum coolant temperature, which is less than 10 °C. Case 5 yields the closest results to the reference values. For the maximum fuel temperature, C~~c~~ase 2 and 5 yield the best results. Again, C~~c~~ases 3 and 4 barely differ.

The low-Mach number model (Case 5) yielded the closest results to the reference solution. However, such a method required a two-level iterative solver. From a computational point of view, the C~~c~~ase 2 model is the simplest method as it does not require an iterative solver. Additionally, the C~~c~~ase 2 model yields the simplest Moltres input file. For these reasons, the rest of the thesis uses the C~~c~~ase 2 model for the fluid flow distribution.

Table 5.8: Mass flow rates [g/s].

Channel	1	2	3	4	5	6	7
Case 1	5.88	10.80	10.85	10.91	11.08	10.80	21.58
Case 2	6.66	10.41	10.41	10.41	10.41	10.41	20.82
Case 3	5.98	10.91	10.91	10.91	10.91	10.91	21.82
Case 4	5.97	10.90	10.90	10.91	10.92	10.90	21.80
Case 5	5.83	10.75	10.81	10.90	11.09	10.73	21.58
Channel	**8**	**9**	**10**	**11**	**12**	**13**	**Half-gap**
Case 1	21.67	21.83	10.88	21.81	22.20	11.10	8.28
Case 2	20.82	20.82	10.41	20.82	20.82	10.41	8.20
Case 3	21.82	21.82	10.91	21.82	21.82	10.91	8.55
Case 4	21.81	21.83	10.91	21.82	21.85	10.92	8.55
Case 5	21.71	21.92	10.84	21.87	22.26	11.08	8.63

Table 5.9: Comparison of the maximum temperatures that the different cases yield.

	Case 1	Case 2	Case 3	Case 4	Case 5
Coolant	1005	994	999	1000	1007
Fuel	1114	1116	1109	1110	1116

Commented [PN19]: remind reader which cases do this here

Commented [PN20]: this is still very good, I'm assuming? maybe put this into context a little

5.2.2 Mesh convergence analysis

The remainder of this chapter intends to solve the full-core problem. This section aims to identify some possible problems introduced by the full-core problem's large mesh size requirement. To do so, t~~T~~his section conducts a mesh convergence analysis of the full-fuel column problem. Figure 5.6 displays the model geometry, and~~.~~ Table 5.10 presents the results. The convergence criteria were 1°C for the maximum coolant and fuel temperatures. The coolant temperature converged for the fifth mesh, but t~~.~~ ~~T~~he fuel temperature did not reach convergence. Further refinement of the mesh was not possible as the simulation memory requirements were too high.

This analysis reveals a potential problem. The high level of detail in our geometry requires ~~a large number of~~many elements in the mesh. In the full-scale problem, the dimensions ~~increase,~~ and the number of elements in the mesh both increase~~do so too~~. Potentially, this method will be unable ~~not be able~~ to solve the three-dimensional, full-scale problem due to a high memory requirement. For this reason, the next section intends to solve the full-scale problem using a two-dimensional, cylindrical model.

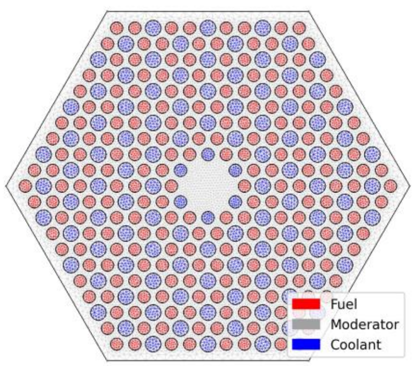

Figure 5.6: Full fuel column model geometry.

Table 5.10: Maximum temperatures.

	Mesh 1	Mesh 2	Mesh 3	Mesh 4	Mesh 5
Number of elements [$\times 10^6$]	1.025	1.306	1.833	2.596	3.006
Number of DoFs [$\times 10^6$]	0.524	0.666	0.932	1.317	1.525
Maximum coolant temperature	1060.41	1062.23	1064.00	1065.13	1065.32
Maximum fuel temperature	1204.49	1217.32	1225.57	1233.44	1234.93

5.3 OECD/NEA MHTGR-350 MW Benchmark: Phase I Exercise 2

This section conducted Phase I, Exercise 2 of the benchmark with Moltres/MOOSE. Phase I, Exercise 2 defines a thermal-fluid standalone calculation. The exercise purpose is to ensure that the thermal-fluid model differences between participants are negligible and will not affect the coupled exercises. The benchmark specifies the power density of each fuel region and defines the mass flow distribution and material properties for four sub-cases:

Commented [PN21]: not sure what this is referencing, but unless the reference specifically doesn't use a comma, I would insert one to improve readability

- Exercise 2a: No bypass flow and fixed thermo-physical properties. The model does not account for the bypass flow, and the thermo-physical properties are constant.
- Exercise 2b: Bypass flow type I and fixed thermo-physical properties. This exercise prescribes the bypass flow distribution, and the thermo-physical properties are constant.
- Exercise 2c: Bypass flow type I and variable thermo-physical properties. This exercise prescribes the bypass flow distribution, and the thermo-physical properties depend on different simulation parameters.
- Exercise 2d: Bypass flow type II and variable thermo-physical properties. This exercise solves the bypass flow distribution through the explicit modeling of the bypass gaps. The thermo-physical properties depend on different simulation parameters.

The exercise requires reporting the average and maximum temperature values of the reflector, Reactor Pressure Vessel (RPV), fuel, moderator, and coolant ~~temperatures~~. It also requires reporting the RPV heat flux and the mass flow rate distribution in the coolant channels and the bypass gaps. These data are helpful to trace the source of possible differences in the primary parameters between participants. Since OECD/NEA did not publish their results for this exercise~~'s results,~~,~~.~~ t~~T~~his section compares Moltres/MOOSE results against INL's benchmark results [114]. It presents only a subset of available data that illustrates the main characteristics of the exercise.

Commented [PN22]: assuming these are all temperatures—if not, specify what quantities the values measure

Commented [PN23]: antecedent needed

Figure 5.7 displays the model geometry. T~~o simplify the simulation of the exercise, t~~he model uses several simplifications in both the axial and radial directions~~.~~ In the axial direction, it does not consider the upper plenum and the outlet plenum, and t~~. T~~he axial boundaries are the top reflector's upper face and the bottom reflector's lower face. T~~. T~~he top reflector's upper face and the inlet coolant flow are at 259 ◦C, while t~~. T~~he bottom reflector's lower face is adiabatic. The outlet coolant uses an outflow boundary condition. In the radial direction, the model does not consider the core barrel and the helium gap. After the outer reflector is the RPV, followed by ~~and after it,~~ the outside air. The outer boundary of the air region is at 30 ◦C.

The core model geometry uses INL's model as the reference design. Nine rings define the solid structures in the core~~,~~ and the other nine rings the coolant flow in the core. We calculated the radii of the rings by preserving the assemblies' volume. The coolant thickness is constant for all the rings and preserves the coolant volume in the core. Table 5.11 presents the material properties. All the graphite regions assume the grade H-451 graphite material properties.

Table 5.12 displays the results. Our model considerably under-predicts the inner reflector rings temperature, while it over-predicts the coolant rings temperature. With the purpose of better understanding this behavior, Figure 5.8 shows the temperature across the reactor on the bottom of the active core (z=200 cm). This figure exposes that the temperatures in the active core are well above the other region temperatures. Although such a behavior is normal, the temperature profile reveals some heat transfer disconnection between the different rings. In other words, the heat transfer from the fuel rings to the rest of the core structures is smaller than the heat transfer to the coolant rings in the active core region. This thermal disconnection causes the reflector temperatures to be too low and the coolant temperatures too high. These results indicate that Moltres model fails to capture some heat transfer mechanisms that INL's model captures. The most notorious difference between the models is the inclusion of the radiative heat transfer. Future works will focus on confirming this supposition and adding the capability to model the radiative heat transfer.

Commented [PN24]: not sure if this is the right word here. maybe "obvious"?

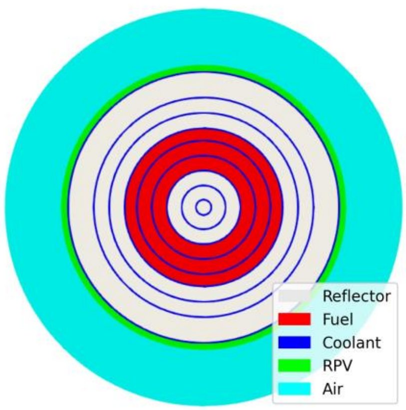

Figure 5.7: Model geometry.

Table 5.11: Problem characteristics.

Parameter	Value	Units	Reference
Fuel compact thermal conductivity	20	W/m/K	[88]
Fuel block thermal conductivity	37	W/m/K	[88]
Graphite thermal conductivity	66	W/m/K	[88]
RPV thermal conductivity	40	W/m/K	[88]
Coolant thermal conductivity	0.41	W/m/K	[88]
Air thermal conductivity	0.068	W/m/K	[88]
Helium density	5.703	$\times 10^{-6}$ kg/cm^3	[91]
Helium heat capacity	5188	J/kg/K	[91]

Table 5.12: First bottom core level average temperatures.

	Reflector			Coolant		
	Ring 1	Ring 2	Ring 3	Ring 4	Ring 5	Ring 6
INL	790	794	802	797	636	673
Moltres/MOOSE	268	313	769	1424	1597	1157

To circumvent this barrier, we developed a second model based on Stainsby's approach [111]. The calculation

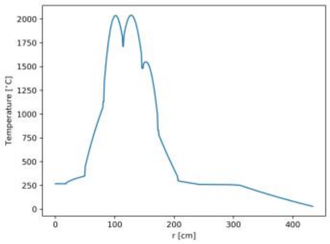

Figure 5.8: Model geometry.

used a global model to obtain the coolant temperature in the core and then a sub-channel model to get the fuel and moderator average temperatures. Figure 5.9 displays the global model geometry. The sub-channel model used half of the unit cell from Section 5.1.2. Three rings defined the solid structures in the global model, and another three defined~~,~~ the coolant flow in the core. We calculated the radii of the rings by preserving the assemblies' volume. The middle ring defines the fuel rings, which encompasses three rings. The coolant ring volumes preserve the coolant volume in each of the fuel rings. The model uses the material properties from Table 5.11.

Figure 5.10 presents the coolant and solid temperatures in the different fuel rings. The temperature is constant in the bottom and top reflector regions. The coolant temperature increases from the top to the bottom of the active core. The highest coolant, fuel, and moderator temperatures are in F~~f~~uel R~~r~~ing 1.

Table 5.13 compares Moltres/MOOSE results to INL's. We focus on the coolant temperature of the different rings. Moltres predicts smaller values in F~~f~~uel ring 1~~, while it~~but predicts higher values in F~~f~~uel R~~r~~ings 2 and 3. For some reason, the global model fails to correctly distribute the heat produced in the fuel rings into the coolant rings~~ the heat produced in the fuel rings~~. A possible cause of this discrepancy is the flat velocity approximation. Section 5.2.1 showed that a flat velocity distribution of the coolant is reasonable in the fuel column model; h~~. H~~owever, one of the assumptions of that model was that the power density is uniform. In this exercise, the power density is not uniform, which could explain~~and that could be causing~~ the discrepancies. Further studies might confirm~~should study~~ the cause of them.

Additionally, Moltres predicts a smaller coolant-to-moderator temperature difference for F~~f~~uel R~~r~~ings 1 and 2. The most considerable discrepancy is in F~~f~~uel R~~r~~ing 1. INL's model coolant-to-moderator temperature difference is 46°C while

Commented [PN25]: so many rings! maybe clear this up a little bit?

Commented [PN26]: temperature of what?

Commented [PN27]: are there multiple temperatures per ring? otherwise, shouldn't this be singular? or is it multiple trials?

Moltres/MOOSE predicts a difference of 30°C. The flat velocity approximation might be again the source of these discrepancies. Finally, the moderator-to-fuel temperature differences from INL and Moltres/MOOSE are close—~~.~~

i~~I~~n F~~f~~uel R~~r~~ing 1, it is 20°C and 22°C for INL and Moltres/MOOSE results, respectively. In F~~f~~uel R~~r~~ing 2, the differences are~~is~~ 16°C and 17°C for INL and Moltres/MOOSE results.

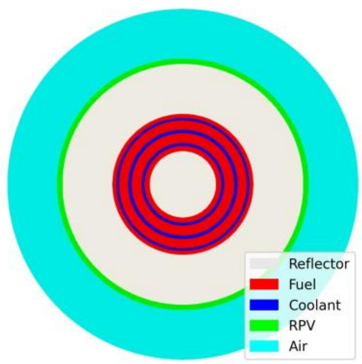

Figure 5.9: Model geometry.

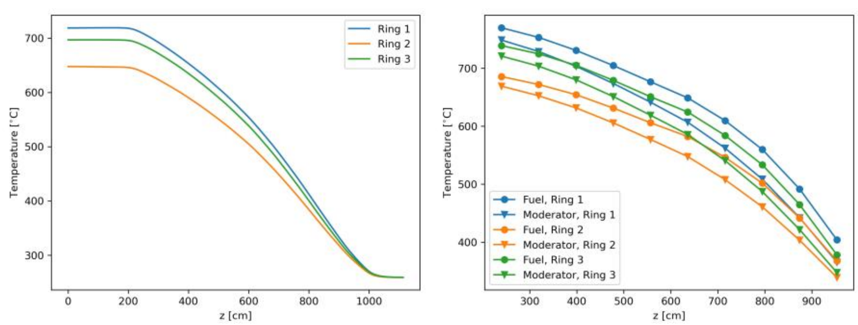

(a) Coolant.

(b) Solid.

Figure 5.10: Axial temperatures.

Table 5.13: First bottom core level average temperatures.

	Fuel ring 1	Fuel ring 2	Fuel ring 3

	INL	Moltres/MOOSE	INL	Moltres/MOOSE	INL	Moltres/MOOSE
Coolant	797	718	636	646	673	696
Moderator	843	748	672	669	Not shown	721
Fuel	863	770	688	686	722	739

5.4 OECD/NEA MHTGR-350 MW Benchmark: Phase I Exercise 3

This section conducted Phase I, Exercise 3 of the benchmark with Moltres/MOOSE. Exercise 3 combines all the data from the first two exercises, in which the participants need to determine a coupled neutronic and thermal-fluids solution. The exercise requires the reporting of the same parameters reported in Exercises 1 and 2 combined. The benchmark specifies the group constants necessary to conduct the exercise. The group constants depend on four state parameters: moderator and fuel temperature and xenon-135 and hydrogen concentration. In addition to these~~is~~ data, the benchmark provides fluence maps to determine the thermal conductivity of graphite.

Two sub-cases compose Exercise 3:

- Exercise 3a: Same thermal-fluids problem definition from Exercise 2c.
- Exercise 3b: Same thermal-fluids problem definition from Exercise 2d.

Section 5.3 solved the thermal-fluids standalone problem using a global and a sub-channel model. Those simulations required running two separate input files, where the output of the global model served as an input to the sub-channel model. Exercise 3 requires modeling the temperature feedback. Using Section 5.3 approach for the temperature feedback would require the fully-coupled simulation of both input files. However, MOOSE framework does not count with the capability to couple these~~is~~ specific problem input files. To solve E~~e~~xercise 3, we created a different model that homogenizes the fuel and moderator materials. The solution did not differentiate between moderator and fuel, thus requiring the simulation of only the global model.

Figure 5.11 presents the model geometry. The model includes 28 fuel and 29 coolant rings. We calculated the radii of the rings by preserving the assemblies' and the coolant volume. The coolant ring pitch is the coolant channel pitch in a fuel assembly. Exercise 3a requires using material properties from Exercise 2c. The simplified model used the material properties from Exercise 2a, as shown in Table 5.11. The benchmark prescribes the group constants of 232 regions in the reactor. Table 5.14 shows what benchmark sub-domains integrate each model region. The model did not include the control rod region (sub-domain 232). The simulations used a three energy-group structure. Table 5.15 indicates what benchmark group numbers integrate each model group. Conducting this exercise required the development of a tool to translate the benchmark group constants to Moltres format. The tool was responsible for homogenizing and collapsing the group constants as well. The problem assumed the same boundary conditions from Section 5.3.

Because Moltres can decouple the neutronics from the thermal-fluid effects, f~~. F~~or the sake of comparison, we conducted the exercise with and without thermal feedback. The calculations without thermal feedback assumed the group constants at 550 ◦C. Figure 5.12 and 5.13 display the results on two arbitrary located lines across the core. The thermal feedback affects the flux, which

Commented [PN28]: I would just copy and paste the problem definition to save your reader from having to scroll all the way back up to see what it is. keep the note that the definitions are repeated though

Commented [PN29]: "come"?

consequently affects the thermal-fluids. The axial flux peak moves towards the reactor top, where the temperatures are lower than the bottom. Thus, the heat production shifts towards the reactor top, and the temperatures near the reactor outlet decrease. The radial flux does not change considerably,; hence the temperature profile does not change much either. The thermal feedback moves the radial temperature profile up because of the heat production shift towards the top.

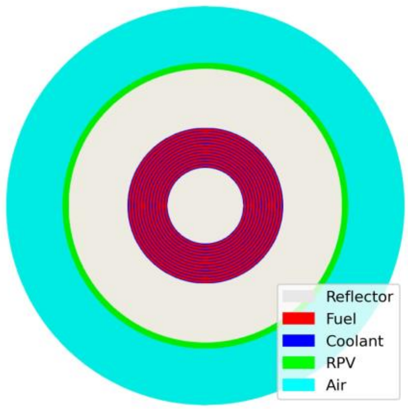

Figure 5.11: Model geometry.

Table 5.14: Homogenization scheme.

Model homogenized region	Benchmark sub-domains
Fuel	1-220
Bottom reflector	221-224
Top reflector	228-231
Inner reflector	225
Outer reflector	226-227

Table 5.15: Energy group condensation scheme.

Model group number	Benchmark group number
1	1-4
2	5-15
3	16-26

5.4.1 Discussion

This section analyzes Moltres' flaws at conducting prismatic HTGR coupled simulations. Moltres' initial development targeted MSRs, allowing it to rely on heterogeneous diffusion calculations. In a heterogeneous solver, each

Commented [PN30]: spell out first instance (I know it's annoying)

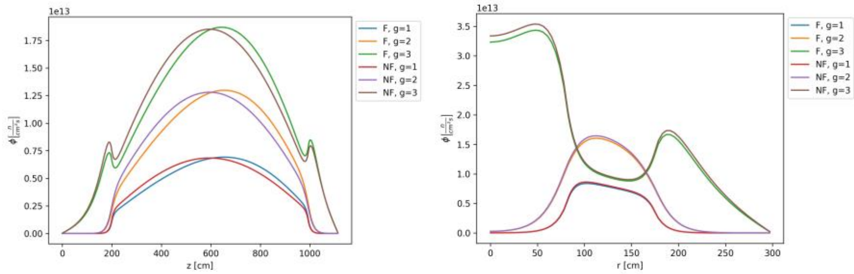

(a) Axial flux over the line at r=85 cm. (b) Radial temperature at z=L/2=556.5 cm Figure 5.12: Flux profiles. F: thermal feedback, NF: no thermal feedback.

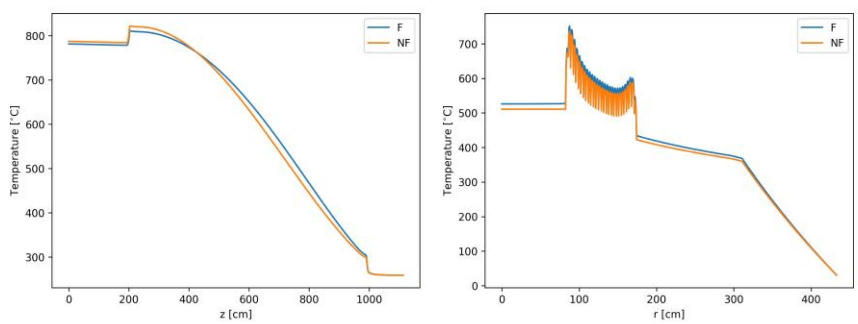

(a) Axial temperature at r=85 cm. (b) Radial temperature at z=L/2=556.5 cm Figure 5.13: Temperature profiles. F: thermal feedback, NF: no thermal feedback. mesh node holds the information of each variable. In an MSR simulation, Moltres defines the neutron flux and the temperature on each node. Each node uses its temperature to compute the thermal feedback on the neutron flux.

As discussed in 4, in a prismatic HTGR simulation, the neutronics calculation requires an assembly-level homogenization of the group constants. Because of the homogenization, a mesh node holds the group constants' combined information from the different materials in the assembly~~-~~— only the fuel and the moderator as the coolant do~~es~~ not contribute considerably. As the

Commented [PN31]: chapter? section?

fuel group constants depended on the fuel temperature, and the moderator group constants depended on the moderator temperature, the thermal feedback depends on both temperatures. Hence, a mesh node should hold both temperatures.

Section 5.4 used a heterogeneous thermal-fluid model to solve the temperature in the reactor. The problem with~~of~~ using a heterogeneous model is that each node only holds the temperature's value in that particular material. A coolant node holds the coolant temperature information and computes the thermal feedback with such information instead of the moderator and fuel temperature. For this reason, Moltres should use the average assembly-level fuel and moderator temperatures instead of the point-wise temperature to compute the thermal feedback.

The thermal-fluids model in Section 5.4 ~~thermal-fluids model~~ homogenized the fuel and the moderator into one material. Consequently, the model does not differentiate the fuel from the moderator temperature. Such homogenization assumes that both the moderator and fuel are in thermal equilibrium, and therefore ~~hence~~ have the same temperature. However, a coupling model cannot correctly calculate the thermal feedback if it does not differentiate between the moderator and the fuel temperatures [25].

We denominate this issue as the 'Homogenization dilemma.' To correctly compute neutronics, the diffusion solver must use homogenized parameters. Simultaneously~~On the other hand~~, to accurately calculate the thermal feedback, the mesh node requires the moderator and fuel temperatures, which require a heterogeneous calculation in the thermal-fluids model.

A thermal-fluid heterogeneous calculation is still valid, but the thermal feedback should use fuel and moderator average temperatures instead. Another approach would be to homogenize the fuel assembly materials and calculate a homogeneous temperature for each material. Such implementation would be more straightforward than using a heterogeneous solver and then averaging the temperatures. An approach with these characteristics is the porous media model. In such a model, the same mesh node holds the fluid and solid temperatures ~~simultaneously~~. However, the use of such a model in the open literature is not always correct, as many articles do not differentiate between moderator and fuel temperatures.

5.5 Conclusions

The preliminary studies focused on the verification of the thermal-fluids model and the validation of the unit cell model. The verification of the thermal-fluids model studied a simplified cylindrical model comparing the Moltres/MOOSE numerical solution to the problem analytical solution— b~~. B~~oth solutions were in agreement. This study set the basis for the unit cell problem set-up. To validate the unit cell model, Section 5.1.2 compared Moltres/MOOSE results to the results of In et al. [53] ~~results~~. The results presented some discrepancies:~~.~~ t~~T~~he outlet coolant and moderator temperatures differed by less than 10°C, while the fuel temperature differed~~s~~ by 22°C. We expected some variability in the results as some of our simulation parameters may have varied~~y~~ from the original study. In's article is missing the materials definition, so ~~and~~ Section 5.1.2 adopted the material properties from Tak et al. [118]. Additionally, In used a chopped cosine power profile while~~and~~ the Section 5.1.2 model simplified the calculation using a uniform power density.

Commented [PN32]: "fuel temperature"?

The following section's focus of the analysis was a one-twelfth section of an HTGR fuel column. To validate the model, Section 5.2 intended to reproduce some of Sato et al. [107] results. Section 5.2 conducted two studies: one with no bypass-gap, and one with a 3mm-bypass-gap. To simplify the analysis, our model adopted the mass flow rates from Sato's article. For both case studies, the maximum temperatures in the coolant and the fuel showed good agreement. Section 5.2 also presented the temperature profile in two of the edges of the geometry. Such an analysis exhibits the effects of the bypass flow on the temperature. The presence of the gap makes the center temperature rise while it reduces the peripheral temperature. The overall consequence is an increase in the temperature gradient inside the column.

The next analysis studied different calculation methods for the mass flow distribution in the fuel column. Section 5.2.1 adopted Sato's mass flow distribution as the reference value and calculated the mass flow distribution using four different methods. From C~~c~~ase 2 to C~~c~~ase 5, the methods' complexity increased~~s~~ as some required iterative solvers. Overall, C~~c~~ase 2 proved to be the simplest method, and its application did not considerably deteriorate the results' accuracy. For that reason, the following studies adopted the C~~c~~ase 2 mass flow distribution method.

Keeping in mind that the ultimate objective of this work is to conduct full-scale simulations, Section 5.2.2 studied the feasibility of extending this methodology to larger meshes. Section 5.2.2 conducted a mesh convergence analysis on the full-fuel column problem. As the model uses the one-dimensional coolant equations, the coolant temperature converges relatively fast compared to the fuel temperature. The fuel temperature did not reach convergence in this analysis, as the mesh discretization increase imposed a high memory requirement on the simulations. This analysis concluded that modeling ~~the~~ thermal-fluids with such a detailed level is computationally too expensive, and it suggests searching for other methods. The following sections adopted a two-dimensional cylindrical model for the full-core analyses.

Section 5.3 described Phase I, Exercise 2 of the OECD/NEA MHTGR-350 MW Benchmark. This exercise encompasses four sub-cases with different definitions of bypass-flow and material properties. The simplest exercise is 2a, as it does not model the bypass flow and provides the definition of the material properties. Section 5.3 used Moltres/MOOSE to conduct Exercise 2a~~it~~. Additionally, the Moltres thermal-fluids model bases its definition on INL's model. As OECD/NEA did not publish this exercise's results, Section 5.3 compared Moltres/MOOSE results to INL benchmark results [114]. The large discrepancies between Moltres/MOOSE and INL results suggest that our model does not capture some heat transfer mechanism that the INL model does. One of the known differences between the models is the inclusion of the radiative heat transfer mechanism. As Moltres does not model that mechanism, it could be the cause of the differences.

Section 5.3 used a global and a unit cell model based on Stainsby's approach [111] to circumvent this drawback. The global model is responsible for calculating the coolant temperature, while the unit cell model focuses on the moderator and fuel temperatures. With this approach, Moltres/MOOSE results were closer to INL results. The results showed some discrepancies, potentially caused by a flat velocity approximation, but indicating overall~~which indicates~~ that some assumption/model

Commented [PN33]: Section __?

Commented [PN34]: maybe specify which results of Sato's you generally wanted to reproduce? otherwise it sounds a little vague

Commented [PN35]: some cases?

Formatted: Font: Not Italic

simplification is not accurate enough. ~~A flat velocity approximation might be the cause of such discrepancies.~~ Further studies should analyze the origin of the discrepancies.

Section 5.4 developed a global model to solve a simplified version of Phase 1, Exercise 3 of the OECD/NEA benchmark. Although the model was simple, it allowed visualizing some of the essential aspects of a prismatic HTGR multi-physics simulation in Moltres. This exercise led to Section 5.4.1, which described some of the flaws found in the model. This exercise also sets the basis for future work that Section 7.2 will introduce.